Three-dimensional mapping and range measurement by means of projected speckle patterns

Javier García,[1,*] Zeev Zalevsky,[2] Pascuala García-Martínez,[1] Carlos Ferreira,[1] Mina Teicher,[3] and Yevgeny Beiderman[3]

[1]Departamento de Óptica, Universitat de València, C/Dr. Moliner, 50, 46100 Burjassot, Spain

[2]School of Engineering, Bar-Ilan University, Ramat-Gan 52900, Israel

[3]Department of Mathematics, Bar-Ilan University, Ramat-Gan 52900, Israel

*Corresponding author: javier.garcia.monreal@uv.es

Received 15 November 2007; revised 27 March 2008; accepted 9 May 2008; posted 9 May 2008 (Doc. ID 89725); published 26 May 2008

We present a novel approach for three-dimensional (3D) measurements that includes the projection of coherent light through ground glass. Such a projection generates random speckle patterns on the object or on the camera, depending if the configuration is transmissive or reflective. In both cases the spatially random patterns are seen by the sensor. Different spatially random patterns are generated at different planes. The patterns are highly random and not correlated. This low correlation between different patterns is used for both 3D mapping of objects and range finding. © 2008 Optical Society of America

OCIS codes: 030.6140, 100.6890, 110.6150.

1. Introduction

Three-dimensional (3D) mapping and ranging are required in computer vision, automation, and optical image processing. Multiple techniques have been devised to accomplish this task [1]. A common principle of many methods is triangulation, using either conventional illumination [2–4] or coherent illumination [5,6]. The main problem with triangulation is the presence of shadows that inhibit the mapping of steep surfaces. Other multiple optical 3D mapping methods include coherence radar [7] and speckle pattern sampling [8]. In both cases the experimental setup is relatively complex due to the interferometric nature of the technique in the first case and the need of a tunable laser in the second case. Holography can also be used for 3D mapping (or, rather, contouring) by the use of multiple wavelengths [9], multiple sources [9], or object displacement between two records [10].

A significant part of the research is based or conditioned by the speckle patterns that happen when coherent light is reflected or transmitted from a rough surface [11–13]. These patterns are the result of interference among scattered wavelets, each arising from a different microscopic element of the rough surface. Speckle patterns have the remarkable quality of each individual speckle serving as a reference point from which changes in the phase of the light scattered from the surface can be tracked. Because of this, speckle techniques such as electronic speckle pattern interferometry (ESPI) have been widely used for displacement measuring and vibration analysis [14–17]. This procedure produces correlation fringes that correspond to the object's local surface displacements between two exposures. In speckle interferometric techniques the changes in the speckle pattern is revealed by adding a coherent reference beam, which converts the subtle variations of phase into a different intensity distribution. It is also possible to analyze the changes in the intensity of the speckle pattern. Under the proper conditions a small rigid body motion of the sample that is illuminated with coherent light will mainly displace the diffracted speckle pattern with little change in the distribution of intensity aside from the shift. This fact enables the use of speckle photo-

0003-6935/08/163032-09$15.00/0

graphy for analyzing displacements and rotations by comparing the shift between two intensity speckle patterns captured in two different situations [11,14,17,18]. It is worth noting that speckle photography and interferometry by themselves can measure the distortion of an object but not its actual 3D shape or range.

For the most part, all the above-referred methods related to speckle patterns used the calculation of the cross-correlation function for the speckle pattern before and after the deformation of an object. All of these methods try to avoid the speckle decorrelation, which is the single most important limiting parameter in measuring systems based on laser speckles, and many efforts have been made to reduce it.

This paper is focused on *using* the decorrelation between different speckle patterns. The method is based on the study of the speckle patterns projected on a certain object. We propose to use a diffuse object, such as a ground glass, to project a speckle pattern onto the object. Inherent changes of the speckle pattern as it propagates will uniquely characterize each location in the working volume. Notably it is the projected speckle pattern that has to be sensed and analyzed, not the speckle pattern produced by the object itself. We apply these speckle pattern changes to three different applications of 3D mapping for both transmissive objects and diffusively reflecting objects and range estimation. We determine the map of a 3D object or its range, observing the differences and similarities of the speckled patterns, when an object is illuminated using light coming from a diffuser. The correlation between the initial and final patterns decreases with the object displacement, so if the displacement is significant, the speckle patterns are statistically uncorrelated. Because of this we first calibrate the region of displacements as a reference to determine the profile of a certain 3D object. To our knowledge, range estimation has never been measured using speckle patterns. In contrast to other pattern projection or triangulation techniques, the 3D resolution in this approach does not depend on the distance or relative angle between the camera and the pattern projector, and thus it is affected by shadowing problems. Moreover the system is robust and reliable as the only interferometric process is concentrated only on the speckle pattern generation, and it does not depend on the object accurate positioning.

2. Theoretical Background of the Projected Speckle Patterns

As stated in Section 1, we are dealing with the speckles projected by the light transmitted by a diffuser. Thus we will need for our applications a description of the speckle pattern in free-space propagation, in particular, the axial and transverse correlation properties. Also, we will use a configuration where a diffuse object illuminated with a speckle pattern is itself imaged by an optical system. Although the fundamental equations are displayed, we refer to the References (mainly [11–13]) for a complete derivation and general discussion.

Let us first consider the description of the speckle patterns and their evolution when the object is axially translated. The derivation is based fully on temporally coherent radiation. This condition can be easily attained if the laser used has a coherence length longer than the maximum path length difference in the setup, a situation that occurs in the later analyzed setups. A ground glass object, $g(x,y)$ (Plane G) normal to the optical axis (see Fig. 1), is transilluminated by a monochromatic parallel beam of laser light of wavelength λ. Speckle patterns are recorded at Plane C, parallel to the object plane. In Plane C, at a distance z from Plane G, the amplitude distribution obtained by the Fresnel diffraction equation is proportional to [19]

$$U(\xi,\eta) = \iint g(x,y) \times \exp\left(j\frac{\pi}{\lambda z}\left[(\xi-x)^2+(\eta-y)^2\right]\right)\mathrm{d}x\mathrm{d}y, \quad (1)$$

and the irradiance is given by

$$I(\xi,\eta) = \left|\iint g(x,y)\exp\left(j\frac{\pi}{\lambda z}\left[x^2+y^2\right]\right) \times \exp\left(-j\frac{2\pi}{\lambda z}\left[\xi x+\eta y\right]\right)\mathrm{d}x\mathrm{d}y\right|^2. \quad (2)$$

To check the change due to propagation, assume that the diffuser is axially translated a distance Δz (see Fig. 1). The irradiance at Plane C is given by Eq. (2), replacing z with $z-z_0$ as [19]

$$I(\xi,\eta) = \left|\int g(x,y)\exp\left(j\tfrac{\pi}{\lambda z}[x^2+y^2]\right) \times \exp\left(j\frac{\pi\Delta z}{\lambda z^2}[x^2+y^2]\right)\exp\left(-j\frac{2\pi}{\lambda z}\left[\xi\left(1+\frac{\Delta z}{z}\right)x + \eta\left(1+\frac{\Delta z}{z}\right)y\right]\right)\mathrm{d}x\mathrm{d}y\right|^2. \quad (3)$$

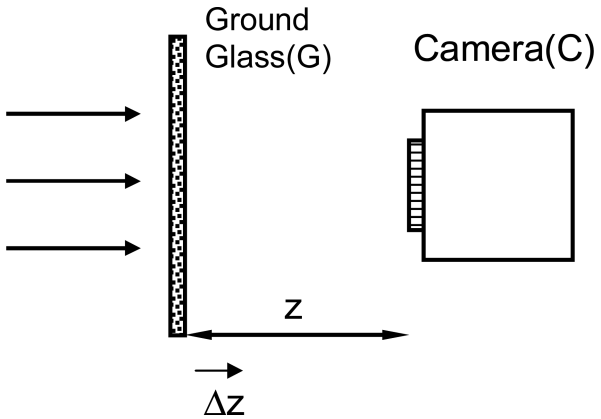

Fig. 1. Variation of the speckle pattern in Plane G when the ground object is axially shifted through Δz.

The interpretation of Eq. (3) shows that the axial translation of g has two main effects [19]. One effect is a radial shift of the speckles linked to the magnification due to geometrical projection from the diffuser screen center to the recording plane. The other effect is a decorrelation of the corresponding speckles due to the term $\exp(j\frac{\pi\Delta z}{\lambda z^2}[x^2+y^2])$.

The first-order statistic of intensity shows that the intensity obeys an exponential law with a mean (and standard deviation) equal to the mean intensity in the case of fully developed speckle. For this probability law to hold, the distribution of phases in the diffuser must be uniform in the $(0, 2\pi)$ interval, which is easily achieved in most ground glass diffusers (as shown in Chap. 4 of Ref. [12]) and is enough that the standard deviation of phases will be in the order of the wavelength.

In the context of this paper, the second-order statistics play a fundamental role. They can be derived from the transverse correlation coefficient of the field at two positions of the pattern [12,13,20] that, aside from constant factors, for the free-space propagation case and for a sufficiently fine grain diffuser is

$$\Gamma_{AT}(\Delta\xi,\Delta\eta) = \iint_{-\infty}^{+\infty} I(x,y) \times \exp\left[-j\frac{2\pi}{\lambda}\left(x\Delta\xi + y\Delta\eta\right)\right]\mathrm{d}x\mathrm{d}y. \quad (4)$$

The correlation function of the intensity between two points separated in the transverse plane by a distance $(\Delta\xi, \Delta\eta)$ is

$$\Gamma_{IT}(\Delta\xi,\Delta\eta) = \bar{I}^2\left\{1 + \left|\frac{\int_{-\infty}^{+\infty} I(x,y)\exp[-j\frac{2\pi}{\lambda}(x\Delta\xi + y\Delta\eta)]\mathrm{d}x\mathrm{d}y}{\int_{-\infty}^{+\infty} I(x,y)\mathrm{d}x\mathrm{d}y}\right|\right\}, \quad (5)$$

where $I(x,y)$ is the intensity in the diffuser (which we take as constant over its extent) and $\bar{I}$ is the mean of the intensity in the output plane. Note that with the proper scaling, the correlation function of intensity is governed by the Fourier transform of the diffuser shape. In our later-described experimental system, we use a circular uniform-intensity diffuser. For this case Eq. (5) reduces to

$$\Gamma_{IT}(r) = \bar{I}^2\left[1 + 2\left|\frac{J_1\left(\frac{\pi\Phi s}{\lambda z}\right)}{\frac{\pi\Phi s}{\lambda z}}\right|\right], \quad (6)$$

where Φ is the diameter of the diffuser, J_1 is the first-kind Bessel function, and $s = \sqrt{\Delta\xi^2 + \Delta\eta^2}$ is the distance between the two sampled points in the transverse plane at distance z from the diffuser. Not so surprisingly the correlation follows the same law (except for additive and multiplicative constants) as the diffraction spot obtained by an imaging system [21]. Eventually the correlation, which is related to the speckle size, is determined by the numerical aperture of the diffuser as seen at the observation plane. At large distances between the samples, the correlation decreases to a background level, corresponding to the autocorrelation of the average intensity value. The speckle lateral size can be obtained by reasoning that inside a given speckle, the correlation must be relatively high. We can take as criterion, analogously to the Rayleigh criterion, the distance where the Airy pattern takes its first minimum. Then we obtain the average transverse size (radius) of the speckle pattern as

$$S_T = 1.22\frac{\lambda z}{\Phi}. \quad (7)$$

As in any resolution criterion, the factor in front of Eq. (7) is somehow arbitrary and depends on the convention for speckle size. It is worth recalling that this is a statistical estimation value, and while it fixes the smallest size of the pattern features, the correlation can often exceed this length.

With respect to the longitudinal extent of the speckles, the problem reduces again to the calculation of the axial correlation function of the intensity [13,20] between two points separated axially by Δz. In this case, with the same assumptions as the transverse case plus the requirement that Δz will be small compared with z, the correlation of intensity results in

$$\Gamma_{IL}(\Delta z) = \bar{I}^2\left[1 + 2\left|\mathrm{sinc}\left(\frac{\Phi^2}{8\lambda z^2}\Delta z\right)\right|\right]. \quad (8)$$

Again the expression, except for the bias corresponding to the correlation of the intensity average, coincides with that of the axial resolution of an imaging system (see Section 8.8 of Ref. [21]). Taking the first null of the sinc function as the criterion to define the speckle size, the half width of the speckle is

$$S_L = 8\lambda\left(\frac{z}{\Phi}\right)^2, \quad (9)$$

where the 8 factor is also subject to the criterion definition. A simplified picture of the speckle pattern in the volume can be visualized by a set of spots at random locations with transverse and longitudinal size given by Eqs. (7) and (9), respectively. Note that the transverse and longitudinal sizes increase linearly and quadratically with the axial distance, respectively. In fact, for large z compared with the transverse dimensions of the experiment, the speckles are elongated along lines radiating from the diffuser center.

The axial and transverse correlations have only a main maximum around the origin, denying the appearance of long distance correlations. This is the

correlation at a long distance compared with the speckle size due only to the average intensity value.

As a main conclusion two speckle patterns taken at lateral or axial distances larger than the transverse or axial speckle sizes [Eqs. (7) and (9)] will be uncorrelated.

The second situation we need to analyze is the imaging configuration in which a diffuse object, coherently illuminated, is imaged by means of a lens. With the condition that both the correlation area on the diffuser and the lens resolution spot size are small compared with the illuminated area, the same equations are valid and a fully developed speckle pattern is obtained in the image plane. We just consider the lens itself a perfect diffuser for speckle characteristics calculations [11,12]. Then the image speckle size is determined by the numerical aperture of the imaging lens or, more directly, by its resolution spot size, which will coincide with the speckle size in the image.

A case where the diffuse object is itself illuminated by a speckle pattern is a particular case of the above-described imaging configuration (eventually, a fixed speckle pattern is a coherent illumination). If the speckle size of the pattern projected onto the object is much larger than the lateral typical size of the surface microstructure, the phase of the projected pattern can be neglected (as it is randomized by the diffuser), and the problem is analogue to a diffusive object with intensity reflectance given by the projected pattern and random phase given by the object microstructure. Of particular interest for this paper is the case where the system resolution spot size on the object is significantly smaller than the projected spot size. Then the image can be seen as the image of the intensity of the projected speckle pattern (unaffected as its resolution is much smaller than the system resolution) modulated by a fine speckle pattern with characteristics given by the lens aperture. We will denote this speckle pattern as the imaging speckle to distinguish it from the primary speckle pattern projected onto the object.

Finally we consider the situation where the lens images a plane at a distance from the diffuser (see Fig. 2). Now the lens makes the coherent imaging of the complex speckle pattern produced by free-space propagation. The spatial frequencies characteristics of the speckle pattern at a distance z from the diffuser in the fully developed speckle case is given by the power spectral density, which is just the Fourier transform of the intensity autocorrelation [Eq. (5)]. Although this is the most common statistical description, we are interested in coherent imaging, so the relevant function is the Fourier transform of the coherence function of the amplitude [Eq. (4)], which is itself the Fourier transform of the diffuser shape. The spatial frequencies are limited by free-space propagation to a cutoff frequency:

$$\nu_c = \frac{\Phi}{2\lambda z}. \tag{10}$$

The coherent transfer function of an imaging system is also a circ function. Therefore, provided that the cutoff frequency of the optical system is larger than that of the speckle pattern, the effect of imaging is only scaling. This is always accomplished with the angle of the diffuser, subtended from the object, being smaller than the angle of lens.

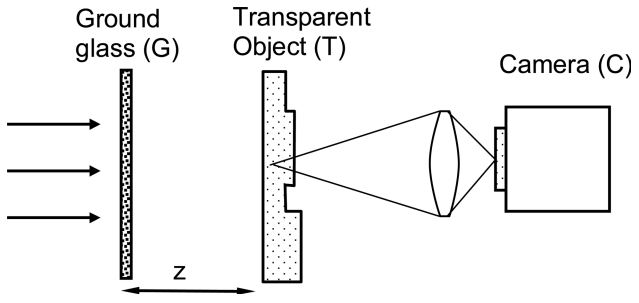

Fig. 2. Setup for transmissive object 3D mapping.

3. Experimental Results for Transmission Thickness Mapping

In Fig. 2 we show the system for the 3D mapping of transparent objects. We project laser light on a small circle on ground glass with an adjustable diameter by means of an iris diaphragm. This illumination creates a speckle pattern in the volume after it, with the illumination distribution depending on the distance from the ground glass. The speckle in a certain plane, at distance z from the ground glass, is imaged on a CCD camera. The diaphragm is adjusted until the size of the speckle on the CCD equals a few pixels, giving a distinct speckle pattern image. The F number of the camera is about 4 (resolution is well below the camera pixel size), so it does not influence the speckle pattern, except for magnification.

The insertion of a transparent plane parallel plate between the camera and the diffuser changes the plane that is imaged in the camera by a distance Δz that depends on the thickness and the index of the plate. As explained in Section 2, the speckles lying in the image plane suffer a decorrelation when the light path increases more than the average length of speckles (S_L) in the z direction [Eq. (9)].

We first calibrate the system by mapping the speckles for the thicknesses of interest. Then, after placing an object composed of patches of plane parallel plates of different thicknesses and imaging the generated speckles pattern, we estimate its 3D mapping. The calibration plates (and those used in the later experiment) are set perpendicular to the optical axis to null the lateral displacement of the speckle pattern. The thickness of the plates can also introduce a change in the scale. Although this effect is inherently taken into account in the calibration process, we use a telecentric lens to reduce the scale changes.

In Fig. 3 we show some of the images used for the calibration of the system. In Fig. 3(a) we present the captured speckle pattern when no transmissive object is placed. In Fig. 3(b) we placed, instead of the

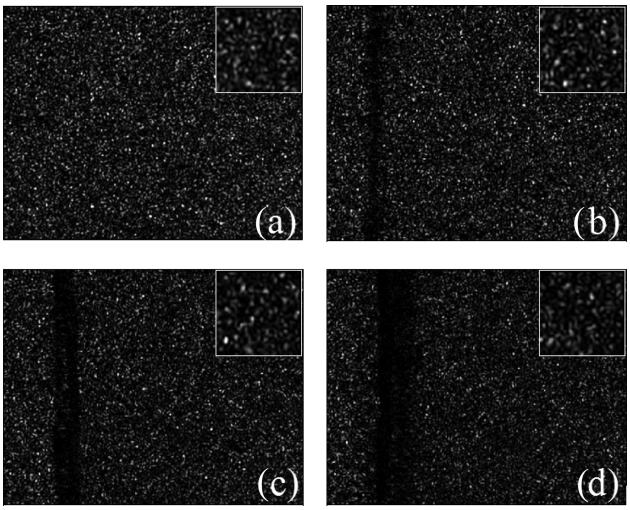

Fig. 3. Calibration reference readout for the transmissive microscopic configuration of 3D mapping using speckles random coding. (a) Speckle pattern without any glass in the optical path. (b) Speckle pattern when one glass slide is inserted into the optical path. (c) Speckle pattern when two glass slides are inserted into the optical path. (d) Speckle pattern when three glass slides are inserted into the optical path. Each slide is 0.5 mm thick. The insets show a magnified portion of the same region for each figure.

object, glass with a thickness of 0.5 mm. In Figs. 3(c) and 3(d) we placed glass with a thickness of 1 mm and 1.5 mm, respectively. As one may see from the obtained images, the patterns are neatly different. The dark vertical lines on the figures are the shadow of the border of the plate, with the left band of the image remaining uncovered (note that it remains unaffected along the figures). This fact reduces the useful area but permits the registering of the subsequent image. The refraction index of the glass used as the inspected object was 1.48. The laser used for the experiment was a He–Ne laser with wavelength of 633 nm. The F number of the diffuser, as seen from the plates plane, is approximately 8. This gives an axial resolution (for full pattern decorrelation) of 300 μm. The additional axial path length introduced by a glass plate is $(n-1)$ times the thickness. Therefore for 0.5 mm of glass we get 240 μm of added optical path, sufficient for producing an almost full decorrelation.

In Fig. 4 we constructed an object containing spatial regions with no glass, glass with a 0.5 mm width, and glass with a 1 mm width. This is denoted in Fig. 4(a) as regions 0, 1, and 2, respectively. Figure 4(b) shows the image captured in the CCD camera. Figure 5 shows the reconstruction results while the reconstruction is done by the absolute value of the subtraction between the captured patterns and the reference patterns (obtained in the calibration process). The dark zones indicate detection. In Fig. 5(a) we subtract the reference pattern of zero width glass in the optical path. In Figs. 5(b) and 5(c), we show the subtraction of the 0.5 mm width and 1 mm width glass slides. As one may see the dark regions appeared where they were supposed to, following the spatial construction of the

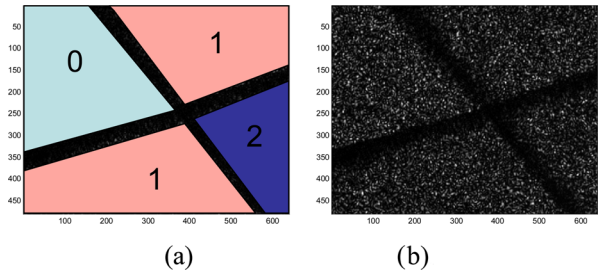

Fig. 4. (Color online) Captured image containing (a) the input pattern that contains a structure of transmissive glasses with widths of zero, one, and two slides (each slide is 0.5 mm thick), and (b) the image captured by the CCD camera when projected with speckles pattern.

object as indicated in Fig. 4(a). Note that the leftmost part of Region 1 [see Fig. 5(b)] is not detected because the calibration plates did not cover this left band.

This method permits the 3D mapping of staircase-type objects. The main restriction on the object is that it must be composed of plane parallel plates. Even a small wedge would divert the light preventing its fall on the lens aperture. A tilt on the object would, in addition to the decorrelation due to the inspection of a different axial plane (it introduces longer optical path), introduce a shift in the pattern that would require a spatial registering of every region separately.

4. Experimental Results for Range Estimation

In this section we use the axial variation of a projected speckle pattern to estimate the axial location of a large object. The experiment of range estimation was performed in reflective configuration in which the ground glass (diffuser) was used to project the speckle pattern on top of a reflective diffuse object, and the reflection was imaged on a CCD camera.

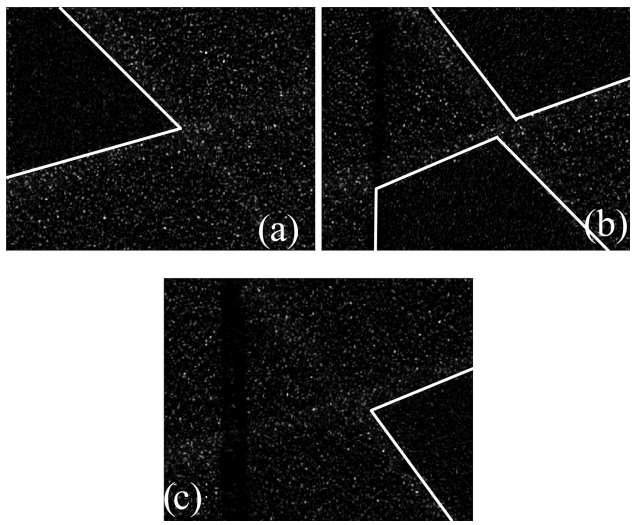

Fig. 5. Segmentation of different regions by absolute value of subtraction between the captured patterns and the reference patterns. (a) Segmentation of Region 0. (b) Segmentation of Region 1. (c) Segmentation of Region 2.

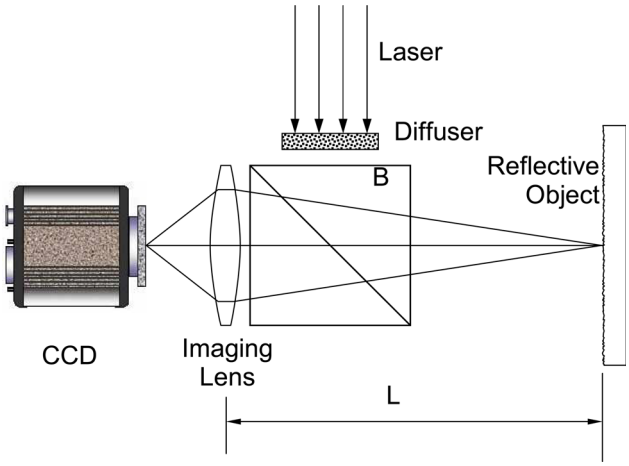

Fig. 6. (Color online) Optical setup for the range estimation.

The system is shown in Fig. 6. Light from a laser source passes through the diffuser. The speckle patterns coming from that diffuser are projected on the reflective object and recorded by a CCD camera. The effective size of the diffuser is adjusted by means of the diaphragm until the image of the projected speckle size is larger than the camera pixel for correct recording. Thus for the case of reflected configuration, the optical parameters are such that the speckle statistics coming from the diffuser (creating the primary projected speckle pattern) are the dominant rather than the influence of the statistics of the object texture itself (creating the imaging speckle pattern as described in Section 2). Such a situation may be obtained, for instance, by choosing the proper diameter of the spot that illuminates the diffuser (since this diameter determines the size of the projected speckles) such that it generates primary speckles that are larger than the secondary speckles generated due to the transmission from the object. That way if the diameter of the imaging lens is larger than the diameter of the effective diameter of the diffuser, the primary speckles are fully seen by the diffraction resolution limit of the camera (the F number), while the secondary speckles, which are smaller, will be partially filtered by the camera since its F number will be too large to contain their full spatial structure. In our experiments we use a lens with an F number of 4, which, for the 532 laser, gives an imaging speckle size of $\sim 2\,\mu$m on the CCD, well below the camera resolution.

For range finding the object was positioned 80 cm away from the CCD camera. The diffuser diameter is set to get an illumination F number of approximately 40, which corresponds to an axial decorrelation length of 6.8 mm according to Eq. (9). To capture the decorrelated speckle patterns, a calibration process was done. It consists of mapping the object by capturing images reflected from 11 planes separated by 5 mm. For quantifying the speckle pattern variations, we use conventional correlation (integral of the product). Initially we record the reference images of the speckle pattern of a diffuse object (a matte white painted plate) at a set of axial distances. We take the 11 reference images, each one separated axially by 5 mm. This set of images is indeed a 3D map of the speckle pattern in the volume of interest. Then we move again on the object in the same axial distance range and obtain the correlation of every image with all the reference set. Therefore we obtain a collection of 11×11 correlation values between the 11 patterns at different distances and the 11 reference images, covering a total axial range of 55 mm.

As an example, in Fig. 7(a) we present the reflected reference speckle pattern that corresponds to a plane positioned 80 cm away from the camera. Note the diagonal black line, which we use as a reference for focusing and positioning. In Fig. 7(b) we depict the autocorrelation between the reflected speckle pattern from a certain plane and its reference distribution obtained in the calibration process. Two main components can be observed in the autocorrelation. On one hand we have the sharp, intense, small peak in the center of the image, which corresponds to the speckle correlation. On the other hand the bulk of the pattern produces a long, broad diagonal correlation pattern owing to the dark line in the sample. The small correlation peak is significantly higher than the broad one. In Fig. 7(c) we present the cross correlation of speckle patterns reflected from two planes separated by 5 mm. Note that the small correlation peak, due to the fine details of the image, has intensity similar to the broad bulk correlation signal, qualitatively showing the decrease of the autocorrelation due to speckle pattern as the two correlated planes are separated axially.

In Fig. 8 we show the range finding results, showing the correlations of each image with the calibration set. As one may see the maxima appear only

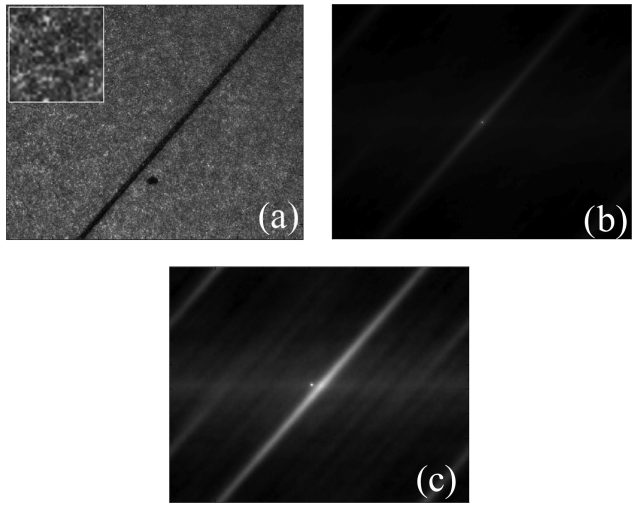

Fig. 7. Reflective speckle patterns used for range finding. (a) The reflected reference speckle pattern corresponds to a plane positioned 80 cm from the camera. The inset is a magnified region. (b) An autocorrelation between the reflected speckles pattern from a certain plane. (c) Cross correlation of speckle patterns reflected from two planes separated by 5 mm.

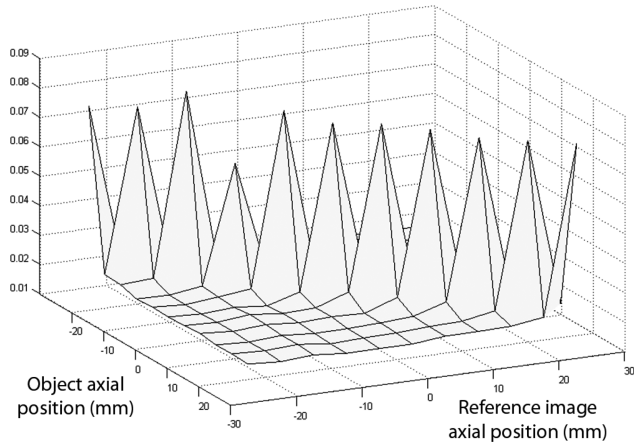

Fig. 8. Range finding results. The cross correlation intensities of the combinations of the reflected patterns from all possible 11 planes positioned at a regular spacing of 5 mm.

at the diagonal (autocorrelation), while the distribution outside the diagonal is small (cross correlation). For further clarification Fig. 8 is actually a cross correlation matrix of 11 × 11, while the indexes (1 to 11) on the horizontal axes represent the plane number and the vertical axis represents the correlation value. The diagonal of the matrix is the correlation value of two images taken at the same distance. Although we have termed these cases as autocorrelation, we want to point out that the correlation is between two very similar images but taken in different instants of time and after relocation of the axial and lateral position. The nondiagonal terms are related to the cross correlation values between the 11 planes. The neat intensity separation between the autocorrelation values and the cross correlation values permits us to identify the distance of the pattern by cross correlation of the pattern at a given unknown distance with the prerecorded patterns.

Note that the process does not depend on the microstructure of the pattern because the ranging is performed on the projected speckle pattern and not on the imaging one. The spectrum of the captured image with only imaging speckle (with uniform illumination of the object) is basically white because the Nyquist frequency of the CCD is much smaller than the typical frequency of the pattern. The effect of the imaging speckle is at pixel level and reduces the signal-to-noise ratio in the projected pattern comparison. Because of this fact the object itself is not relevant, provided that it is a fine diffuse object. As a confirmation of this fact, the region of the test plate used for the experiments was not the same in the calibration images as in the test image, thus having a different microstructure in the field of view.

5. Experimental Results of the Three-Dimensional Mapping of Reflective Objects

In Section 4 we used the large area correlation for the depth determination. In this section we propose the use of local correlation to map the depths of small regions in a 3D object. We use a calibration procedure similar to the previous one, capturing the speckle pattern projected on a white painted plate at a set of axial positions that cover the working volume. In this case the correlation is not performed for the full image as in the range finding case, but rather we perform a correlation of the local windows of the object with the same region of each of the calibration patterns to give the final 3D mapping. Note that in this case the projected speckle pattern is capture from the surface of completely different objects during the calibration (reference plane diffuse plate) and during the mapping (the object itself).

A basic parameter that we need for the procedure is the minimum size of the correlation window that will separate the autocorrelation value of the speckle pattern from the cross correlation between two windows with uncorrelated (by depth changes) speckles. A analytical treatment is possible (see Chap. 4 in Ref. [12] for a similar problem), but the solution is generally not in a closed form and may be influenced by additional factors such as the digitalization noise. Therefore we prefer to perform a preliminary test to check the minimum window size. We use one of the reference images obtained by projecting the speckle pattern on a plane plate. We perform autocorrelations and cross correlations between windows chosen at random positions in the field. The mean and the variance of the correlations are obtained for 500 positions. The results are plotted in Fig. 9, showing the mean values and the confidence interval for one standard deviation for the autocorrelation for different circular window sizes normalized to the speckle size. As can be seen in the figure, the two values can be separated from window sizes exceeding 3.5 times the speckle size. In the following experiment we used a running window size of 10 pixels.

In Fig. 10 we show the results that were obtained for a 3D object made up with toy building blocks. The

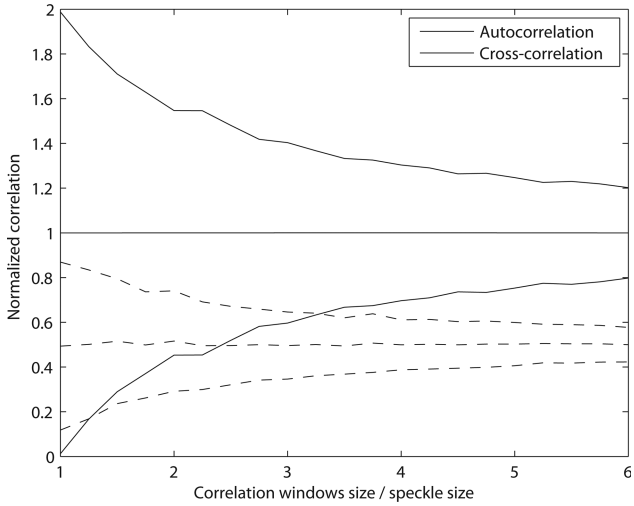

Fig. 9. Variation of the mean and confidence interval at one standard deviation for the autocorrelation and cross correlation of varying size of circular regions.

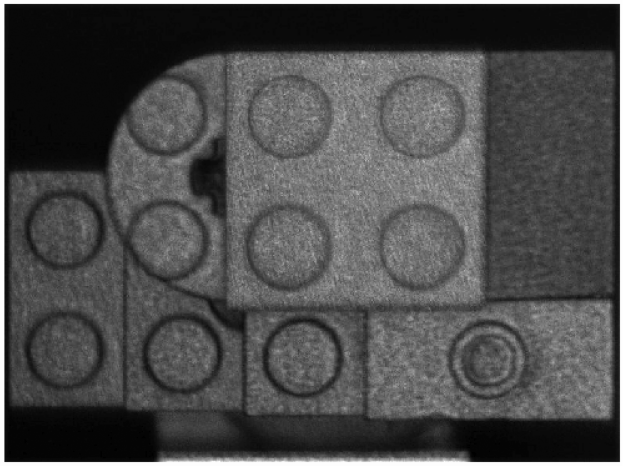

(a)

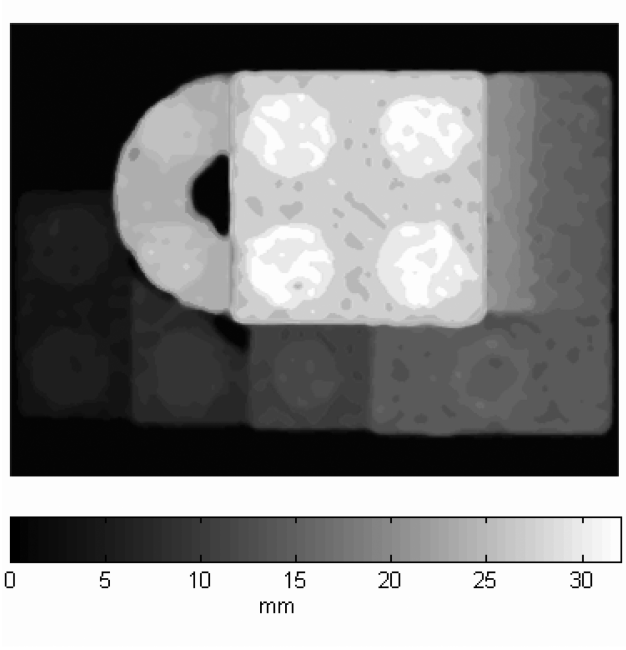

(b)

Fig. 10. (a) Object illuminated with the projected speckles pattern. (b) 3D reconstruction.

object occupied a volume of $40 \times 25 \times 30$ mm. As a main advantage over most 3D mapping methods, the proposed procedure has virtually no shadowing because the illumination and image recording are performed from the same location.

6. Conclusions

We have presented the optical usage of speckles for the thickness mapping of transparent objects, 3D diffuse object mapping, and range estimation. The key concept is to use a ground glass that produces a pattern that changes with the depth inherently by free-space propagation. The projected pattern decorrelates when it is sampled at two different positions separated either axially or transversely. The computation of the correlation between the actual pattern as projected or transmitted by the object and a set of calibration images allow the determination of the 3D location or shape of the object. The concept has also been applied to 3D mapping by computing the correlation between the object and the reference images on a running window of small size. Despite the relatively small resolution, the system is robust and almost independent on the characteristics of the object. The projection of the speckle in the volume can be made from a small and thus solid and stable system because it comprises only the laser and the diffuser. A significant advantage of the method is the absence of shadowed area and high configurability. Experimental results present the verification of the proposed directions.

This work was partially supported by the FEDER funds Spanish Ministerio de Educación y Ciencia under the project FIS2007-60626.

References

1. F. Chen, G. M. Brown, and M. Song, "Overview of three-dimensional shape measurement using optical methods," Opt. Eng. **39**, 10–22 (2000).
2. M. Sjödal and P. Synnergren, "Measurement of shape by using projected random patterns and temporal digital speckle photography," Appl. Opt. **38**, 1990–1997 (1999).
3. H. Farid and E. P. Simoncelli, "Range estimation by optical differentiation," J. Opt. Soc. Am. A **15**, 1777–1786 (1998).
4. J. S. Chahl and M. V. Srinivasen, "Range estimation with a panoramic visual sensor," J. Opt. Soc. Am. A **14**, 2144–2151 (1997).
5. R. E. Brooks and L. O. Heflinger, "Moiré gauging using optical interference patterns," Appl. Opt. **8**, 935–939 (1969).
6. G. Indebetouw, "Profile measurement using projection of running fringes," Appl. Opt. **17**, 2930–2933 (1978).
7. T. Dressel, G. Hausler, and H. Venzhe, "Three dimensional sensing of rough surfaces by coherence radar," Appl. Opt. **31**, 919–925 (1992).
8. G. R. Hallerman and L. G. Shirley, "A comparison of surface contour measurements based on speckle pattern sampling and coordinate measurement machines," Proc. SPIE **2909**, 89–97 (1997).
9. B. P. Hildebrand and K. A. Haines, "Multiple-wavelength and multiple-source holography applied to contour generation," J. Opt. Soc. Am. **57**, 155–162 (1967).
10. N. Abramson, "Holographic contouring by translation," Appl. Opt. **15**, 1018 (1976).
11. J. C. Dainty, *Laser Speckle and Related Phenomena*, 2nd ed. (Springer-Verlag, 1989).
12. J. W. Goodman, *Speckle Phenomena in Optics* (Roberts and Co., 2006).
13. J. W. Goodman, *Statistical Optics* (Wiley, 1985).
14. H. M. Pedersen, "Intensity correlation metrology: a comparative study," Opt. Acta **29**, 105–118 (1982).
15. J. A. Leedertz, "Interferometric displacement measurements on scattering surfaces utilizing speckle effects," J. Phys. E **3**, 214–218 (1970).
16. P. K. Rastogi and P. Jacquot, "Measurement on difference deformation using speckle interferometry," Opt. Lett. **12**, 596–598 (1987).
17. M. Sjödahl, "Calculation of speckle displacement, decorrelation and object point location in imaging systems," Appl. Opt. **34**, 7998–8010 (1995).

18. M. Sjödahl, "Electronic speckle photography: increased accuracy by non-integral pixel shifting," Appl. Opt. **33**, 6667–6673 (1994).
19. J. A. Mendez and M. L. Roblin, "Relation entre les intensities lumineuses produites par un diffuseur dans deux plans paralleles," Opt. Commun. **11**, 245–250 (1974).
20. L. Leushacke and M. Kirchner, "Three dimensional correlation coefficient of speckle intensity for rectangular and circular apertures," J. Opt. Soc. Am. A **7**, 827–833 (1990).
21. M. Born and E. Wolf, *Principles of Optics*, 7th (expanded) ed. (Cambridge University, 1999), Chap. 8, p. 491.